Production and structural analysis of membrane-anchored proteins in phospholipid nanodiscs

Kolio Raltchev[a][b], Joka Pipercevic[a][b], and Franz Hagn*[a][b]

Abstract: Structural studies on membrane-anchored proteins containing a transmembrane (TM) helix has been hampered by difficulties in producing these proteins in a natively folded form. Detergents that are required to solubilize the hydrophobic TM helix usually destabilize the soluble domain. Thus, TM helices are removed for structural studies, which neglects the pivotal role of a membrane on protein function. Here, we present a versatile strategy for the production of this protein class attached to phospholipid nanodiscs. By inserting the TM-helix into nanodiscs and a subsequent SortaseA-mediated ligation of the soluble domain, membrane-anchored BclxL could be obtained in a folded conformation. We show that this strategy is suitable for high-resolution structure determination as well as for probing membrane location by NMR. This method will be applicable to a wide range of membrane-anchored proteins and will be useful to decipher their functional role in a native membrane environment.

Despite recent advances in their functional characterization and structure determination[1], membrane proteins are still poorly understood. Traditionally, integral membrane proteins are extracted from the membrane by or refolded into detergents[2]. This approach requires extensive screening for suitable buffers and detergents, however, often yields homogenous preparations of folded and functionally active membrane proteins. The situation is more heterogeneous for membrane attached proteins. If a fatty-acid membrane anchor mediates this interaction, co-expression with a modifying enzyme, such as myristoyl-transferase[3] that adds a myristoyl chain to e.g. a G-protein alpha subunit, is well established, yet often leads to poor yields. The most challenging case are membrane attached proteins that contain a transmembrane helix for anchoring. In principle, these proteins could also be extracted from cell membrane after production but the yields are usually very low and the presence of detergents often leads to incorrectly folded proteins.

The solution for studying this protein class so far is to remove the TM helix and study the soluble domain alone. This has been done for members of the Bcl2 family of proteins[4], for tumor necrosis factor[5], transforming growth factor[6], integrins[7], T-cell receptor subunits[8], and a whole variety of other ectodomains. Many of these proteins contain disulfide bridges and thus often need to be refolded from inclusion bodies for structural studies. Refolding yields are often low and the presence of a hydrophobic TM helix would make it almost impossible to obtain correctly folded protein. These proteins are all composed of a TM helix and one or more soluble domains, located either at the C- or N-terminus. The Bcl2 family of proteins is a prominent member of this class. Most Bcl2 proteins are anchored to the outer mitochondrial membrane and the balance between pro- and anti-apoptotic Bcl2 proteins determines whether the cell is driven into apoptosis[9]. Furthermore, Bcl2 proteins tend to insert into the membrane and thus are highly detergent sensitive[10] (Fig. S1). The pro-apoptotic members Bax and Bak form large oligomeric membrane pores that enable exit of pro-apoptotic proteins from the mitochondrial intermembrane space to induce caspase-mediated apoptosis[11]. Anti-apoptotic members, like BclxL, bind to the pro-apoptotic members and inhibit pore formation[12]. Under certain conditions, these proteins get cleaved by caspases and insert into the membrane by them-selves to form pro-apoptotic pores[13]. Overall, due to the lack of a membrane environment in previous structural studies, the mechanism of membrane insertion and the initial location of BclxL on the membrane surface is still poorly understood from a structural perspective as only full-length BclxL is suitable to study conformational changes and its functional features in a native membrane environment.

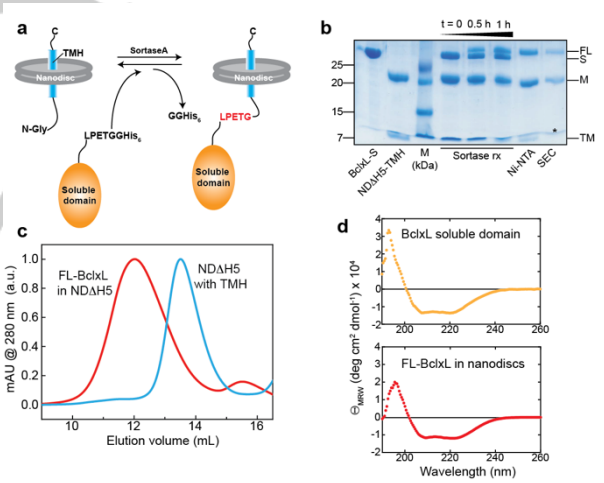

Figure 1. SortaseA-mediated production of full-length BclxL in nanodiscs. (a) Schematic overview of the ligation strategy. (b) SDS-PAGE of the components for as well as a time-series of the ligation reaction and the purification of the product. (c) SEC profiles of FL-BclxL and nanodiscs containing the TMH only. (d) Far-UV CD spectra of BclxL-solu and FL-BclxL. FL: full-length; S: soluble domain; TM: transmembrane helix; ND∆H5: nanodiscs formed with MSP1D1∆H5.

Here, we present a versatile and easy SortaseA-based method to produce membrane-anchored proteins attached to phospholipid nanodiscs for NMR structural studies. Nanodiscs[14] have been previously optimized for NMR structural studies of integral membrane proteins[15] and further covalent circularization of the membrane scaffold protein that encircles a patch of lipid bilayer yielded exceptional size homogeneity[16]. We use BclxL as

[a] M.Sc. Kolio Raltchev, M.Sc. Joka Pipercevic, Prof. Dr. Franz Hagn
Bavarian NMR Center at the Department of Chemistry and Institute for Advanced Study
Technical University of Munich
Lichtenbergstrasse 4, 85747 Garching, Germany
E-mail: franz.hagn@tum.de

[b] M.Sc. Kolio Raltchev, M.Sc. Joka Pipercevic, Prof. Dr. Franz Hagn
Institute of Structural Biology
Helmholtz Zentrum München
Ingolstädter Landstrasse 1, 85764 Neuherberg, Germany

Supporting information for this article is given via a link at the end of the document.

a prominent membrane-anchored protein and show that high-resolution NMR structure determination is possible for this protein class. Furthermore, we obtained structural information on the location of the soluble BclxL domain relative to the membrane surface. This toolset will be useful to investigate structural and functional features of Bcl2 proteins in a realistic membrane environment, as well as study the structure of a large variety of other membrane-associated proteins.

In a previous study, full-length BclxL was incorporated into nanodiscs using detergent solubilization of a protein precipitate[17]. In our hands, this approach did not result in properly folded BclxL, which was the main motivation to develop an alternative method to produce membrane attached full-length BclxL that can be easily expanded to other members of this protein class. Our strategy was to divide BclxL into two parts, the TM helix (TMH) and soluble domain (BclxL-solu). The TMH can be solubilized in detergent micelles and incorporated into phospholipid nanodiscs. The TMH incorporated into nanodiscs was then ligated to the soluble domain using SortaseA enzyme[18]. With this strategy, we were able to obtain natively-folded and membrane-attached BclxL.

First, we designed suitable protein constructs where a SortaseA recognition motif was fused to the C-terminus of BclxL-solu and where GB1[19] was added to the N-terminus of the TMH (Fig. S2). Next, we established and optimized SortaseA-mediated ligation of nanodisc-incorporated TMH with BclxL-solu (Fig. 1a) and obtained overall ligation yields of up to 85%. The ligation reaction was completed after 30-60 min at room temperature using an optimized SortaseA variant showing enhanced catalytic efficiency[20]. Purification of the product could be achieved by Ni-NTA and size exclusion chromatography (SEC) (Fig. 1b, SI Methods) and ligation was verified by MALDI-TOF MS and dynamic light scattering (Fig. S3). The SEC profile (S200 column, 24 mL bed volume) of full-length (FL-) BclxL in nanodiscs compared to the TMH alone in nanodiscs shows significant differences, where FL-BclxL elutes at 11.8 mL and the TMH at 13.5 mL, indicative of a larger hydrodynamics radius of the first (Fig. 1c). The marked increase in size can be explained by the location of BclxL-solu outside the nanodisc. We used far-UV CD-spectroscopy to probe the secondary structure content in FL-BclxL in nanodiscs as compared to BclxL-solu (Fig. 1d). The CD data of the nanodisc sample was corrected for the presence of the MSP protein. These data show that BclxL retains its α-helical secondary structure while present at the membrane surface.

Successful nanodisc incorporation could be shown by the appearance of a band for the MSP protein and the TMH peptide in SDS-PAGE. (Fig. 1b). Furthermore, we moved on to characterize the TMH in nanodiscs with NMR. We recorded 2D-[^{15}N;^{1}H]-TROSY spectra at 45°C that contained 24 out of the expected 31 resonances in the TMH. We then conducted 3D-TROSY-HNCA and HNCACB experiments on *U*-[^{2}H,^{13}C,^{15}N]-labeled TMH in nanodiscs formed with MSP1D1ΔH5 and deuterated d_{54}-DMPC/DMPG lipids in a 3:1 ratio (Fig. 2). The quality of these spectra was sufficient to obtain assignments of all visible resonances in the 2D experiment. Furthermore, a comparison between TMH in DPC micelles and nanodiscs clearly shows that the linewidth of the resonances in the 2D-[^{15}N;^{1}H]-TROSY spectrum is larger in nanodiscs than in detergent micelles, indicating the formation of a larger particle (Fig. S4a). In addition, the use of a lipid bilayer instead of a detergent micelle leads to pronounced chemical shift perturbations, presumably due to changes in the local structure and electronic environment (Fig. S4b).

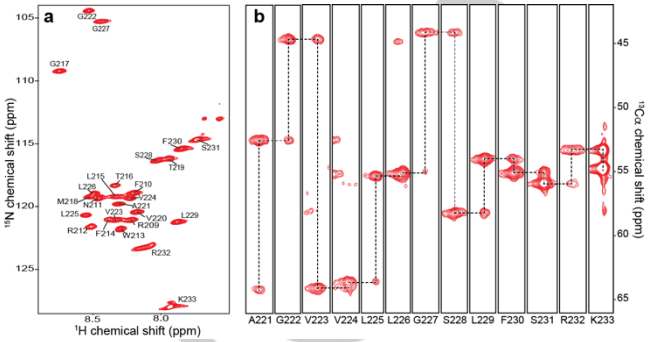

Figure 2. Backbone resonance assignment of BclxL-TMH in nanodiscs. The quality of the (a) 2D-[^{15}N;^{1}H]-TROSY and (b) 3D-TROSY-HNCA strips is sufficient for a detailed NMR analysis. Sequential connections are indicated by broken lines.

Next, we were interested in probing the functional properties of ligated FL-BclxL by isothermal titration calorimetry (ITC) with a PUMA BH3 peptide that is known to bind to the canonical BclxL BH3 binding groove with nanomolar affinity[21]. As a reference, we used BclxL-solu alone, that has been used for previous experiments in the literature. As can be seen in Fig. 3a, the affinity of PUMA BH3 for BclxL is almost identical in BclxL-solu (K_D = 66 nM) and in FL-BclxL (K_D = 56 nM). In addition, all other thermodynamic parameters (ΔG, ΔH, ΔS) that characterize the binding mode are very similar in each case. This behavior

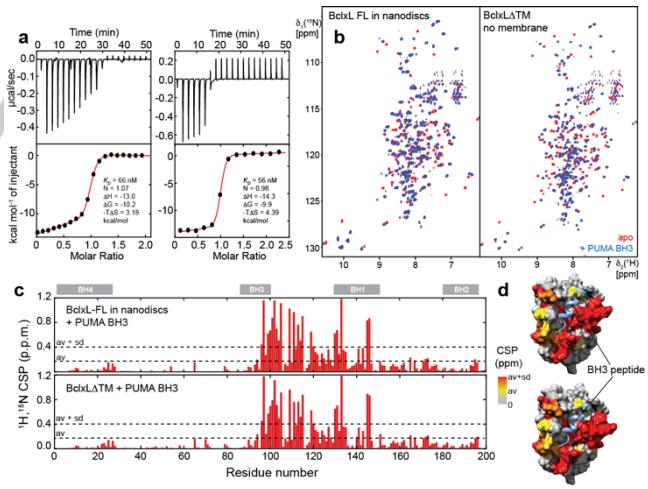

Figure 3. Comparison of binding affinity and mode be-tween FL-BclxL and BclxL-solu. (a) Isothermal titration calorimetry (ITC) probing binding of a PUMA BH3 peptide to BclxL-solu and FL-BclxL. (b) NMR titration of both proteins with PUMA BH3 peptide followed by 2D-[^{15}N;^{1}H]-TROSY experiments. (c) CSP values plotted against residue number in each case and (d) CSP values color-coded on the structure of BclxL. av: average CSP value, sd: standard deviation

indicates that the structure of the soluble domain in the SortaseA-ligated full-length protein attached to phospholipid nanodiscs is in the native ligand-binding competent state, in contrast to studies in detergent micelles[10]. In order to obtain further information on the

binding mode in a per-residue resolution, we used NMR chemical shift perturbation (CSP) experiments (Fig. 3b). The extracted CSP values are almost identical in both cases, further corroborating that the binding mode is identical (Fig. 3c,d), which means that the soluble domain is properly folded even in close proximity to a membrane surface.

Another interesting feature that can be probed with NMR is the location of a protein relative to the lipid bilayer membrane. Therefore, we incorporated Gd^{3+}-chelated lipids (Gd^{3+}-DTPA-DMPE) into our nanodiscs. The paramagnetic relaxation enhancement (PRE) of Gd^{3+} leads to NMR signal attenuation in a distance-dependent manner and thus can be used to probe membrane proximity, as recently shown for small GTPases[22]. Due to the fact that BclxL is able to inhibit pore formation of pro-apoptotic Bcl2 proteins Bax and Bak by binding to their BH3 domains, one might argue that the soluble domain with its functional BH3 peptide binding site is required to be in close proximity to the membrane. We therefore produced nanodisc incorporated FL-BclxL where BclxL-solu is segmentally labeled with ^{2}H and ^{15}N in presence or absence of Gd^{3+}-DTPA-DMPE in the assembled nanodiscs. We then analyzed the signal intensities in 2D-[^{15}N;^{1}H]-TROSY experiments in each case, i.e. calculated relative intensities as compared to the reference sample without Gd^{3+}. As can be seen in Fig. 4a and c, these data indicate that the BH3 binding site in BclxL is in close proximity to the membrane. Only signals originating from residues in this region are significantly broadened and show reduced intensity. This suggests that the face of BclxL-solu that harbors the BH3 binding site is loosely attached to the membrane, awaiting binding partners. The same NMR experiments were also performed with nanodisc-incorporated ^{2}H,^{15}N-labeled BclxL-TMH, which can be used to further confirm membrane insertion but which can also serve as a positive control, as strong attenuation of signals in the TMH that are located in the lipid head-group region are expected. As shown in Fig. 4b and d, this is exactly the case. Only the central hydrophobic residues in BclxL-TMH are not affected by line broadening, whereas the intensity of the more peripheral residues is clearly reduced. In both cases color-coding from grey to red was used to visualize the PRE-effects (Fig. 4c, d).

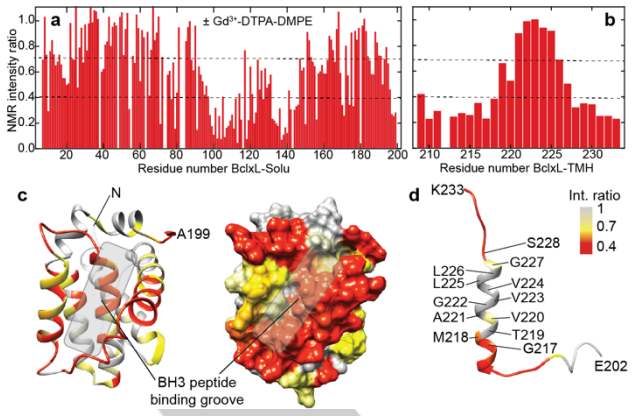

Figure 4. Paramagnetic relaxation enhancement (PRE) to probe membrane location of BclxL. (a) PRE-intensity plot of NMR signals of FL-BclxL (^{2}H,^{15}N-BclxL-solu) in nanodiscs containing Gd^{3+}-DTPA-DMPE. (b) PRE-intensity plot of BclxL-TMH in Gd^{3+}-DTPA-DMPE nanodiscs. (c) and (d) Color-coding of the PRE-data on the structures of BclxL-solu (c) and TMH (d).

In order to demonstrate the application of the presented approach for high-resolution NMR structure determination of this protein class, we recorded 3D-NOESY experiments on the isotope labeled BclxL-TMH as well as isotope-labeled BclxL-solu ligated to the unlabeled TMH in nanodiscs. The quality of the NOESY data (Fig. S5) is suitable for extracting distance restraints for subsequent structure determination. This has been done for the TMH, where residues 214-229 show clear amide-amide NOE cross-peaks that are indicative of a α-helical secondary structure (Fig. S5a). This data was used to calculate a structural model of the TMH in nanodiscs. We also recorded a 3D-^{15}N-edited NOESY experiment on the segmentally-labeled soluble domain. The spectrum clearly shows that pairwise distance restraints can be extracted (Fig. S5b). Due to the fact that the 2D-[^{15}N;^{1}H]-TROSY spectra of BclxL-solu and FL-BclxL are very similar, we did not perform a full NOE-based structure calculation in this case. Instead we recorded HN residual dipolar couplings (RDCs) of ^{2}H,^{15}N-labeled BclxL-solu in the full-length framework incorporated into nanodiscs at 40°C in presence of 8 mg/mL Pf1 phage (Asla Biotech, Riga, Lativa). The resulting HN-RDCs were used to refine the structure of BclxL-solu (1lxl.pdb[23]). We found an excellent agreement of experimental and back-calculated HN-RDCs (R=0.94, Q=0.19) (Fig. 5a) and thus assume that the structure of the soluble domain in FL-BclxL is not significantly altered as compared to the soluble domain in isolation.

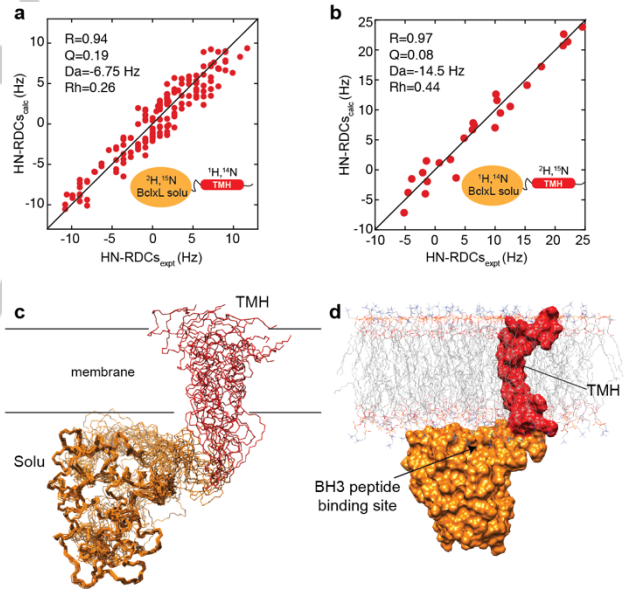

Figure 5. Structure refinement of FL-BclxL using residual dipolar couplings (RDCs). Correlation between experimental and back-calculated backbone amide RDCs of the soluble (a) and the TMH (b) of BclxL using segmentally-labeled BclxL as indicated in the inset. (c) Relative orientation between both structural elements in the RDC-refined structure. (d) The main binding site on BclxL is located right next to the membrane surface, ready to interact with pro-apoptotic Bcl2 proteins. Da and Rh, magnitude and rhombicity of alignment tensor; R: correlation coefficient, Q: quality factor

Furthermore, we were able to obtain HN-RDCs of FL-BclxL in nanodiscs, where only the TMH is labeled with ^{2}H and ^{15}N (Fig. 5b). With these data, we could refine the structure of the TMH to obtain very good agreement between experimental and back-

calculated RDCs (R=0.98, Q=0.08). The magnitude of the HN-RDCs of both parts are significantly different, where the soluble domain that is tumbling in solution outside the membrane shows values between -12 and +12 Hz and the TMH that is located in the nanodisc lipid bilayer membrane shows values between -6 and +24 Hz. This difference in the observed HN-RDCs can be caused by the specific orientation of the HN bond vectors relative to the magnetic field or by enhanced dynamics of the soluble domain as compared to the TMH, as summarized in a previous review[24]. Analysis of the order tensor eigenvalues (S_{zz},S_{xx},S_{yy}, for details, see Fig. S6) in both cases shows that the order is increased in the TM helix (higher values of the tensor eigenvalues) as compared to the soluble domain, consistent with a model that the TMH is stably attached to the membrane, conferring alignment characteristics of a nanodisc. The soluble domain is only loosely attached to the membrane surface and thus exhibits relative motions relative to the nanodisc, leading to reduced alignment and a lower magnitude of HN-RDCs. Therefore, it was necessary to use two separate alignment tensors for subsequent structure refinement. In order to obtain a structural model of FL-BclxL in and on a lipid bilayer membrane, we combined NOEs, RDCs and chemical shift information for NMR structure calculation. The resulting structural bundle clearly shows that the relative orientation between the TM helix and the soluble domain is fairly well defined (Fig. 5c). The soluble domain docks against the membrane surface with its BH3 peptide binding groove oriented toward the lipid bilayer membrane surface (Fig. 5d), which seems reasonable as BclxL needs to be kept in a binding competent state once pro-apoptotic Bax or Bak proteins insert into the membrane to form pores and expose their BH3 binding site. In line with these observations, CD-detected thermal unfolding experiments (Fig. S7) showed that BclxL is less stable if located at a membrane surface than in solution. The apparent melting point of BclxL-solu is 80°C, whereas the membrane-bound form already unfolds at 64°C. The known unfolding behavior of the membrane scaffold protein (MSP1D1ΔH5) takes place at 88°C[15a], which is well-separated from the first unfolding transition. This lowering in thermal stability can be explained by the known tendency of BclxL to insert into the membrane, which can be triggered by low pH and high temperature[25]. These previous studies have been conducted with the soluble domain of BclxL alone, which underestimates the effect of local proximity of a membrane surface. As the hydrophobic binding groove of BclxL is oriented towards the membrane surface, adjacent lipid molecules might bind and destabilize the folded domain upon heating.

The presented data describe a robust method for the production of membrane-associated proteins containing a TM helical anchor. In particular, for structural studies, this membrane protein class is very difficult to produce in a functional form and high yield. Our SortaseA-based ligation approach introduces a 5-residues LPETG peptide. In order to minimize the potential impact of this sequence modification, a native sequence motif that shows some similarity should be modified and appropriate binding or functional assays should be used to assess functionality. In our case, we could not see any difference in the binding affinity to the PUMA BH3 peptide between the non-mutated soluble domain and the slightly modified FL-BclxL. For biological assays, BclxL is commonly being produced as a GST-fusion protein. However, for nanodisc incorporation this approach did not yield NMR spectra of sufficient quality for further structural investigations (Fig. S8), where only the loop regions of the folded domain of BclxL could be observed, in stark contrast to protein obtained with our SortaseA-based approach. Another recently published method to produce FL-BclxL without any fusion protein for NMR studies[17] did not result in soluble protein in our hands, emphasizing the difficulty in dealing with this protein class. The herein developed methodology as well as the structural insights into BclxL on a membrane surface will enable further investigations on how this protein acts as an inhibitor of pore formation of pro-apoptotic Bax and Bak. In general, this method can be widely applied for the production and structural characterization of a whole variety of membrane-anchored ectodomains that reside at the cell membrane and require a membrane environment for their cellular function using NMR but also (cryo-) electron microscopy.

Experimental Section

Experimental details on protein constructs, protein production and purification, nanodisc assembly, SortaseA-mediated protein ligation, analytical methods and NMR-based structure determination is provided in the supporting information.

Acknowledgements

This work was supported by the Deutsche Forschungsgemeinschaft (SFB1035, project B13), the Helmholtz Center Munich, the Helmholtz Society and the Center for Integrated Protein Science Munich (CIPSM). We thank the Bavarian NMR Center for providing high-field NMR instrumentation and Markus Fleisch (TUM) for assistance with DLS experiments. The backbone resonance chemical shift assignments of BclxLTMH in nanodiscs as well as the structural coordinates of the 20 lowest-energy structures have been deposited at the BMRB (ID: 27316) and wwPDB (ID: 6F46.pdb) databanks.

Keywords: NMR • apoptosis • nanodiscs • membrane • SortaseA

[1] R. M. Bill, P. J. F. Henderson, S. Iwata, E. R. S. Kunji, H. Michel, R. Neutze, S. Newstead, B. Poolman, C. G. Tate, H. Vogel, *Nat Biotech* **2011**, *29*, 335-340.
[2] A. Pandey, K. Shin, R. E. Patterson, X.-Q. Liu, J. K. Rainey, *Biochemistry and Cell Biology* **2016**, *94*, 507-527.
[3] R. J. Duronio, E. Jackson-Machelski, R. O. Heuckeroth, P. O. Olins, C. S. Devine, W. Yonemoto, L. W. Slice, S. S. Taylor, J. I. Gordon, *Proc Natl Acad Sci U S A* **1990**, *87*, 1506-1510.
[4] A. M. Petros, E. T. Olejniczak, S. W. Fesik, *Biochimica et Biophysica Acta (BBA) - Molecular Cell Research* **2004**, *1644*, 83-94.
[5] M. J. Eck, S. R. Sprang, *Journal of Biological Chemistry* **1989**, *264*, 17595-17605.
[6] T. P. J. Garrett, N. M. McKern, M. Lou, T. C. Elleman, T. E. Adams, G. O. Lovrecz, H.-J. Zhu, F. Walker, M. J. Frenkel, P. A. Hoyne, R. N. Jorissen, E. C. Nice, A. W. Burgess, C. W. Ward, *Cell* **2002**, *110*, 763-773.
[7] J.-P. Xiong, T. Stehle, B. Diefenbach, R. Zhang, R. Dunker, D. L. Scott, A. Joachimiak, S. L. Goodman, M. A. Arnaout, *Science* **2001**, *294*, 339.
[8] K. C. Garcia, M. Degano, R. L. Stanfield, A. Brunmark, M. R. Jackson, P. A. Peterson, L. Teyton, I. A. Wilson, *Science* **1996**, *274*, 209.
[9] M. H. Harris, C. B. Thompson, *Cell Death Differ* **2000**, *7*, 1182-1191.

[10] aJ. A. Losonczi, E. T. Olejniczak, S. F. Betz, J. E. Harlan, J. Mack, S. W. Fesik, *Biochemistry* **2000**, *39*, 11024-11033; bT. J. Malia, G. Wagner, *Biochemistry* **2007**, *46*, 514-525.
[11] D. Westphal, G. Dewson, M. Menard, P. Frederick, S. Iyer, R. Bartolo, L. Gibson, P. E. Czabotar, B. J. Smith, J. M. Adams, R. M. Kluck, *Proceedings of the National Academy of Sciences* **2014**, *111*, E4076-E4085.
[12] P. E. Czabotar, G. Lessene, A. Strasser, J. M. Adams, *Nat Rev Mol Cell Biol* **2014**, *15*, 49-63.
[13] E. A. Jonas, J. A. Hickman, M. Chachar, B. M. Polster, T. A. Brandt, Y. Fannjiang, I. Ivanovska, G. Basanez, K. W. Kinnally, J. Zimmerberg, J. M. Hardwick, L. K. Kaczmarek, *Proc Natl Acad Sci U S A* **2004**, *101*, 13590-13595.
[14] I. G. Denisov, Y. V. Grinkova, A. A. Lazarides, S. G. Sligar, *Journal of the American Chemical Society* **2004**, *126*, 3477-3487.
[15] aF. Hagn, M. Etzkorn, T. Raschle, G. Wagner, *Journal of the American Chemical Society* **2013**, *135*, 1919-1925; bF. Hagn, G. Wagner, *J Biomol NMR* **2015**, *61*, 249-260; cF. Hagn, M. L. Nasr, G. Wagner, *Nat Protoc* **2018**, *13*, 79-98.
[16] M. L. Nasr, D. Baptista, M. Strauss, Z. J. Sun, S. Grigoriu, S. Huser, A. Pluckthun, F. Hagn, T. Walz, J. M. Hogle, G. Wagner, *Nat Methods* **2017**, *14*, 49-52.
[17] Y. Yao, L. M. Fujimoto, N. Hirshman, A. A. Bobkov, A. Antignani, R. J. Youle, F. M. Marassi, *J Mol Biol* **2015**, *427*, 2262-2270.
[18] H. Mao, S. A. Hart, A. Schink, B. A. Pollok, *Journal of the American Chemical Society* **2004**, *126*, 2670-2671.
[19] P. Zhou, G. Wagner, *Journal of biomolecular NMR* **2010**, *46*, 23-31.
[20] I. Chen, B. M. Dorr, D. R. Liu, *Proc Natl Acad Sci U S A* **2011**, *108*, 11399-11404.
[21] aF. Hagn, C. Klein, O. Demmer, N. Marchenko, A. Vaseva, U. M. Moll, H. Kessler, *J Biol Chem* **2010**, *285*, 3439-3450; bA. V. Follis, J. E. Chipuk, J. C. Fisher, M.-K. Yun, C. R. Grace, A. Nourse, K. Baran, L. Ou, L. Min, S. W. White, D. R. Green, R. W. Kriwacki, *Nature chemical biology* **2013**, *9*, 163-168.
[22] M. T. Mazhab-Jafari, C. B. Marshall, P. B. Stathopulos, Y. Kobashigawa, V. Stambolic, L. E. Kay, F. Inagaki, M. Ikura, *Journal of the American Chemical Society* **2013**, *135*, 3367-3370.
[23] S. W. Muchmore, M. Sattler, H. Liang, R. P. Meadows, J. E. Harlan, H. S. Yoon, D. Nettesheim, B. S. Chang, C. B. Thompson, S. L. Wong, S. L. Ng, S. W. Fesik, *Nature* **1996**, *381*, 335-341.
[24] J. R. Tolman, K. Ruan, *Chem Rev* **2006**, *106*, 1720-1736.
[25] M. Vargas-Uribe, M. V. Rodnin, A. S. Ladokhin, *Biochemistry* **2013**, *52*, 7901-7909.

Entry for the Table of Content

COMMUNICATION

We here introduce an efficient SortaseA-based method for the production of membrane anchored proteins attached to phospholipid nanodiscs for structural and functional studies in a native membrane environment. We apply this method to the anti-apoptotic protein BclxL and demonstrate that high-resolution structure determination by NMR is possible for this protein class.

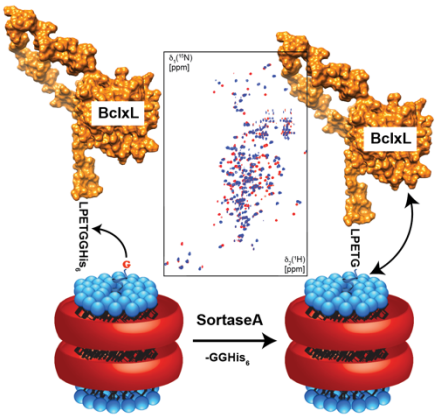

*Kolio Raltchev, Joka Pipercevic and Franz Hagn**

XXX – YYY
Production and structural analysis of membrane-anchored proteins in phospholipid nanodiscs